J Mater Sci (2006) 41:7341–7352
DOI 10.1007/s10853-006-0792-2

Preparation and properties of nitrile rubber/montmorillonite nanocomposites via latex blending

M. A. Kader · K. Kim · Y.-S. Lee · C. Nah

Received: 10 March 2005 / Accepted: 2 December 2005 / Published online: 19 September 2006

Abstract The nitrile rubber (NBR)/unmodified montmorillonite (Na-MMT) clay nanocomposites were prepared by latex blending method followed by melt mixing of compounding ingredients by using two-roll mill. The X-ray diffraction (XRD) studies showed an increase in the basal spacing and broadening of peak corresponding to crystal structure of Na-MMT indicating the formation of intercalated/exfoliated clay layers in the NBR matrix. Increase in clay content of nanocomposite increased the XRD peak height due to the formation of many of clay tactoids at higher loading. The transmission electron microscopy (TEM) strengthened the XRD finding by showing the presence of intercalated/exfoliated morphology of clay platelets having good dispersion. The modulus and tensile properties of the nanocomposites were improved with addition of Na-MMT which is proportional to clay concentration. The retention of tensile properties of aged nanocomposites, with all clay concentration, was superior to either pure NBR and carbon black filled NBR composite. The dynamic mechanical analysis showed proportional increase in storage modulus analogous to Na-MMT loading at all the temperature ranges due to the confinement of polymer chains between the clay layers. Nanocomposites with different proportions of clay showed a decrease in tan δ_{max} peak height with a shift towards higher temperature indicating the reduction in the segmental mobility of polymer chain. A linear model was proposed to correlate the influence of Na-MMT content on storage modulus of nanocomposites. Differential scanning calorimetry indicated a linear increase in glass transition of nanocomposites which is proportional to clay loading. Thermogravimetric analysis revealed a small improvement in the thermal stability of nitrile rubber/clay nanocomposites.

M. A. Kader · K. Kim · C. Nah (✉)
BK-21 Polymer BIN Fusion Research Team, Chonbuk National University, 664-14, Duckjin-dong, Duckjin-gu, Jeonju, Chonbuk 561-756, South Korea
e-mail: cnah@chonbuk.ac.kr

M. A. Kader
Department of Polymer Technology, Crescent Engineering College, Vandalur, Chennai 600-048, India

Y.-S. Lee
School of Environmental and Chemical Engineering, Chonbuk National University, Jeonju 561-756, South Korea

Introduction

Recently, polymer–clay nanocomposites (PCN) have attracted significant attention due to their outstanding mechanical properties even at a considerably lower clay concentration [1]. The high aspect ratio silicate clay layers having nanometer scale size in the nanocomposites greatly reduce gas and liquid permeability by imposing a tortuous pathway to the permeant [2, 3]. Enhanced chemical and fluid resistance and flame retardancy of polymer/layered clay nanocomposites benefit from the hindered diffusion pathway [4, 5]. Among many clay minerals, sodium montmorillonite (Na-MMT) has been recognized as one of the potential candidates for improving physico-mechanical properties of PCN. A detailed description of the crystal structure, stacking of layers, and exchangeability of the interlayer cations of MMT are available in the literature

[6–8]. The formation of intercalated and/or exfoliated PCN can greatly be improved by treating the Na-MMT with organophilic agents such as quaternary ammonium salt, phosphonium salts, etc. through ion exchange reaction. However, the use of Na-MMT without organic treatment can greatly reduce the cost of nanocomposites. Recently, many review articles on PCN, covering various aspects in this field, were published [9–11]. The polymer/clay nanocomposites can generally be prepared by most common methods such as in situ polymerization, solution and melt mixing and latex blending. Among these methods, latex blending has many advantages due to its simplicity, less capital investment and environmentally less harmful nature of the process. Considerable works on the preparation of rubber/clay nanocomposites by latex method are reported by many researchers [12–16]. Latex blending involves mixing of rubber latex and a clay aqueous dispersion under some specified mixing conditions, to enhance good dispersion, and then co-coagulating the mixture by adding an electrolyte. The mechanism of nanocomposite formation in the latex stage may proceed through two different path ways. In the first type, the aqueous dispersions of clay swells and the rubber molecule can penetrate into the inter-galleries of the clay and thus makes good dispersion. In the second mechanism, the latex particles are located between the well separated clay layers in the aqueous clay dispersion during vigorous mixing. A ''separated'' rubber/clay nanocomposites, whose structures are similar to those of intercalated/exfoliated polymer–clay nanocomposite, can be formed upon co-coagulation [13, 14]. The rubber/layered clay nanocomposites can be considered as alternative material for the highly filled conventional rubber compounds due to many advantages. The nanocomposites derived from nitrile rubber (NBR) have been investigated extensively with respect to morphological and rheological properties [17], mechanical and dynamic mechanical properties [18], gas barrier properties [19, 20], fracture behavior [21] and cure properties [22]. Furthermore, Okada et al. [23] reported that only 10 phr of layered clay is sufficient to achieve similar tensile properties, which can be obtained by adding as much as 40 phr carbon black to NBR. Moreover, the aging properties of rubber–clay composite in presence of organic modifier indicated good retention of mechanical properties [24].

Earlier, we carried out investigation on cure kinetics of NBR/organoclay nanocomposites prepared from melt mixing process [25]. However, no report has been published with respect to the preparation of NBR/clay nanocomposites through latex blending method using unmodified clay. In the work, we explored a novel method of preparation of NBR/montmorillonite nanocomposites using latex blending method to prepare nanocomposite from untreated MMT. The latex blending technique with a set of mixing condition favorable for the formation of intercalated/exfoliated nanocomposites was used. Additionally, until now, there is no report on the accelerated aging performance of rubber/clay nanocomposites. We made an attempt to study the influence of clay on aging resistance of NBR. The influence of clay loading on the dynamic mechanical properties was also investigated and a model for calculation of storage modulus from the clay concentration was proposed to find out the influence of clay content.

Experimental

Materials

Sodium montmorillonite with cationic exchange capacity (CEC) of 119 mequiv/100 g was obtained Kunimine Industries, Japan. The NBR latex (acrylonitrile content: 34%) was obtained from Hyundai Petrochemical Co., Korea. Carbon black (N220 type, Lucky Carbon Black, Korea) was used as conventional filler for comparison purpose. Other rubber compounding ingredients were obtained from local manufacturer.

Preparation of NBR–clay nanocomposites

The clay aqueous suspension was prepared by dispersing 20 g of clay in 600 cm^3 distilled water at 80 °C for 24 h under high stirring. The NBR latex was then mixed with the clay dispersion and stirring was continued at a relatively higher speed at 60 °C for 3 h. The mixture was then coagulated using dilute solution of dichloroacetic acid (DCA, 0.001 M) as an electrolyte. The pH of the resulting mixture was around 4. The coagulant was then washed several times with distilled water, tested for pH (≈5–6) and dried in an air oven at 80 °C for 18 h. Subsequently, the compounding ingredients for vulcanization (conventional cure system) were mixed with this in an open two-roll mill. The compounds were prepared with the clay content of 2, 5, and 10 phr. The compounding formulation is given in Table 1. The carbon black was used to prepare conventional composite in order to compare the physicomechanical properties with nanocomposites. The compounds were cured at 160 °C in a heated press (Carver, USA) under a pressure of 5 MPa for the

Table 1 Formulation, cure characteristics and mechanical properties of NBR and its conventional and nanocomposites

Sample	NBR	NBR-M2	NBR-M5	NBR-M10	NBR-CB50
NBR (by weight)	100	100	100	100	100
Na-MMT (by weight)	0	2	5	10	-
N220 (CB)	–	–	–	–	50
t_{s2}	8.92	6.31	4.77	4.19	2.62
T_{90}	18.5	17.2	16.4	17.9	11.1
M_L	1.3	2.3	4.1	5.1	4.8
M_H	26.5	37.2	49.0	55.6	44.4
$\Delta S(M_H - M_L)$	25.2	34.9	44.9	50.5	39.6
Hardness (shore A)	49	63	69	75	71
100% modulus (MPa)	1.84	3.06	5.2	9.25	3.7
300% modulus (MPa)	–	11.4	14.2	19.7	15.7
Tensile strength (MPa)	4.5	15.2	19.7	21.5	25.7
Elongation at break (%)	284	349	401	343	456
Tear energy (kJ/m^2)	1.7	4.2	7.3	8.6	13.8
Solvent swelling, V_r (%)	345	271	197	153	208

All compositions contain (in phr): ZnO—5.0; Stearic acid—2.0; sulfur—2.0, NS (accelerator)—1.0

optimum cure time, which was determined from an oscillating disk rheometer (ODR-2000, Alpha Technology, USA) to make a rubber sheet of thickness <2 mm.

Characterization and testing

X-ray diffraction pattern (XRD) between 2 and 10° (2θ) were obtained at a scan rate of 2°min^{-1} on a diffractometer (Rigaku 2500PC, Japan) with CuKα radiation at a generator voltage of 40 kV, and a generator current of 40 mA and wave length of 0.154 nm at room temperature. Transmission electron microscopy (TEM) images were taken from cryogenically microtomed ultra thin section of specimen using a ZEISS EFTEM (model: EM912 OMEGA H-800) operating at 120 kV.

In mechanical properties, dumbbell-shaped specimens were cut from the molded rubber sheets for the measurement of tensile properties. Modulus, tensile strength and elongation at break were obtained from stress–strain curves obtained from a tensile tester (Lloyds, UK) at room temperature according to the procedure described in ASTM D412. Six specimens were used per sample and the data is reported for the average values. Hardness was determined by hand-held Shore-A Durometer (Asker, Kobunshi Keiki Co. Ltd) with the samples having more than 6 mm thickness. The tear test was performed using trousers tear test method. The rubber strips of dimensions $100 \times 25 \times 1$ mm^3 bonded with textile reinforcement along the edges parallel to strips (to minimize the deformation of legs during testing) were used. The tearing rate was set at 50 mm/min. Values of tearing energy, G_c, were calculated from the measured force, F, by the following simple equation [26]:

$$G_c = \frac{2(\alpha_s)^2 F}{\omega} \quad (1)$$

where α_s is the linear swelling ratio (unity in this study), and ω is the torn width.

Scanning electron microscopy (JEOL, JSM 6400, USA) was used to analyze the fracture morphology of torn surface of the rubber sample.

Solvent swelling of cured rubber compounds was carried out in methyl ethyl ketone (MEK), a solvent for NBR. Samples were weighed (w_1) before immersion into MEK at 25 °C. After 72 h, when equilibrium swelling was reached, the swollen samples were removed, wiped dry and again weighed (w_2). The degree of swelling was calculated using the following equation.

$$\text{Swelling}\ (\%) = \frac{w_2 - w_1}{w_1} \times 100 \quad (2)$$

The dynamic mechanical analysis was carried out in a DMA instrument (GABO 127, Germany) in the temperature range: –50 to 150 °C at a frequency of 1 Hz; with a pre-strain of 1%; under tension mode. Accelerated aging of the tensile specimens was carried out in an air-circulating oven at 104 °C for various time periods up to 10 days. The retention of mechanical properties was calculated as follows:

$$\text{Retention}\ (\%) = \frac{[\text{Property}]_{\text{aged}}}{[\text{Property}]_{\text{unaged}}} \times 100 \quad (3)$$

The differential scanning calorimetry (DSC) was performed with TA instruments (DSC model 2910) under nitrogen atmosphere at a heating rate of 10 °C min^{-1} in the temperature range of –60 and 80 °C

to determine the glass transition temperature. Thermogravimetric analysis (TGA, TA Q50, TA Instruments) measurement was carried out in the temperature range of 30 °C to 700 °C with a heating rate of 10 °C/min under the flow of nitrogen to analyze the thermal stability of samples.

Results and discussion

X-ray diffraction pattern

The structure of polymer–clay nanocomposites (PCN) has traditionally been elucidated using XRD and transmission electron microscopy (TEM). XRD is the most commonly used technique to identify intercalated structures due to the periodic arrangement of the silicate layers both in the pristine and the intercalated states. The repetitive multilayer structure is well preserved in intercalated structures, allowing the interlayer spacing for determination. Intercalation of polymer chains between the clay layers usually increases the interlayer spacing, which results in shifting of the XRD peak toward lower angles. Figure 1a shows the diffraction patterns of 001 plane in montmorillonite (Na-MMT), DCA treated Na-MMT, NBR and NBR/Na-MMT nanocomposites with various Na-MMT loadings. The interlayer spacing of Na-MMT was observed at $2\theta = 7.37^{o}$ (d spacing calculated from Bragg's law = 1.20 nm) whereas DCA treated Na-MMT showed the peak at $2\theta = 6.27$ (d_{001} = 1.41 nm). For NBR/Na-MMT samples, the peak appeared at 2θ value of 6.35^{o} (d_{001} = 1.39 nm) with a decrease in peak intensity compared to pristine Na-MMT. This indicates a small gallery expansion of about 0.2 nm in the layered clay in Na-MMT/DCA and NBR/Na-MMT samples. The increase in basal spacing of Na-MMT by DCA is due to absorption of DCA through hydrogen bonding between carboxylic group of DCA and the hydroxyl group in Na-MMT. This increase in basal spacing is smaller than that of organoclay having more than eight carbon atom [18, 27]. The similarity in d-spacing between rubber/layered clay samples and Na-MMT/DCA suggests that the monolayer rubber molecule might have intercalated into the clay layers. However, in addition to the presence of a peak, there was an increase in breadth of the peak which extent towards lower 2θ values for nanocomposites. Such broadening of the diffraction peak suggests that the occurrence of partial exfoliation as the crystal size decrease. According to the Scherrer relation, $B = K\lambda/L\cos\theta$ where K is a numerical proportionality constant, the width of the peak B (measured by full width at half maximum, FWHM) is inversely proportional to the coherence length of the scattering entities, L and therefore reflects the coherent order of the silicate layers. As the angular width of the reflection increases, the length over which coherency existence decreases. Therefore, the observed change in FWHM of the composite suggests that the diffusion or insertion of rubbery polymer chains disrupt the layer structure of the silicate crystallite so that layers become exfoliated or more irregularly spaced from each other. The dispersion of clay layers in NBR can be found as a bimodal structure representing both intercalated and exfoliated state. However, higher clay loading would lead to poorer dispersion with the formation of more clay aggregates in the rubber matrix. The extent of intercalation/exfoliation can only

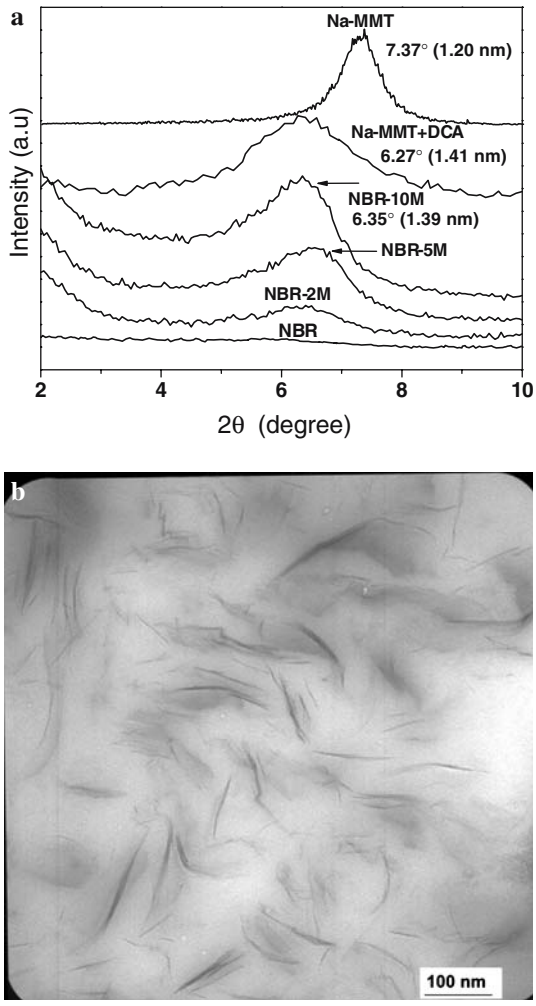

Fig. 1 (**a**) Wide angle XRD for Na-MMT, NBR and NBR/Na-MMT nanocomposites with varying proportions of Na-MMT (Na-MMT/DCA is also included for comparison). (**b**) High magnification TEM image of NBR/Na-MMT intercalated/exfoliated nanocomposite (loading of Na-MMT = 5 phr)

be detected using TEM, which characterizes the nanostructural features of the polymer/clay hybrids. Figure 1b shows a TEM microphotograph of NBR-5 M having a random orientation of clay stacks with only few platelets of MMT as well as randomly distributed single platelets. These smaller stacks gave rise to a peak in the XRD pattern. It is inferred from both XRD data and TEM image that the Na-MMT was uniformly dispersed in the NBR matrix at lower loading. However, at a considerably higher loading, Na-MMT formed small aggregates with few platelets of clay layers. Nevertheless, it should be mentioned here that the Na-MMT used in this study was an unmodified one without the addition of any organic modifier or a combatibilizer.

Cure behavior

The vulcanization characteristics of NBR, NBR/CB and NBR/layered clay nanocomposites having different concentration of Na-MMT are presented in Table 1. The effect of Na-MMT on the rheographic profile obtained at 160 °C is illustrated in Fig. 2. The addition of Na-MMT resulted in an appreciable increase in the minimum torque (M_L) which can be related to an increase in the viscosity of composites. This behavior may be attributed to the formation partially exfoliated nanostructure of clay platlets which form physical crosslink with rubber matrix and thereby immobilize part of rubber chains leading to an increase in viscosity. The increase in the viscosity of 50 phr N220 filled NBR may be due to chemical interaction between carbon black and rubber through reinforcing action. The difference between maximum (M_H) and minimum torques, M_H-M_L, increased significantly in presence of both MMT and CB indicating the influence of the fillers on the crosslink density. The effect of the fillers on the crosslink density could also be estimated from swelling experiments. As presented in Table 1, there was a linear decrease in the V_r values with the addition of Na-MMT. Interestingly, the degree of crosslinking (from both torque and swelling data) of 5 and 10 phr MMT filled NBR was higher than that of 50 phr N220 filled system indicating greater reinforcing nature of nanoscale clay particles through confinement of polymer chains adjacent to clay layers. Concerning the scorch resistance, the addition of Na-MMT decreased the scorch time (t_{s2}) in a linear fashion due to the better heat distribution in the NBR matrix around the clay particles having large surface area which enhanced the crosslinking [17]. The influence of normal amount of strong acid used in the coagulation of latex on scorch time is not high [28]. Moreover, very small amount of dilute DCA was used during coagulation of NBR and there the concentration of residual DCA in the coagulated rubber was very low due to repeated washing with distilled water. If any free DCA was present, it might be neutralized by ZnO used in the formulation. The optimum cure time (t_{90}) was not affected much by increasing the clay loading probably because of faster cure in the early stage of crosslinking than in the latter stage.

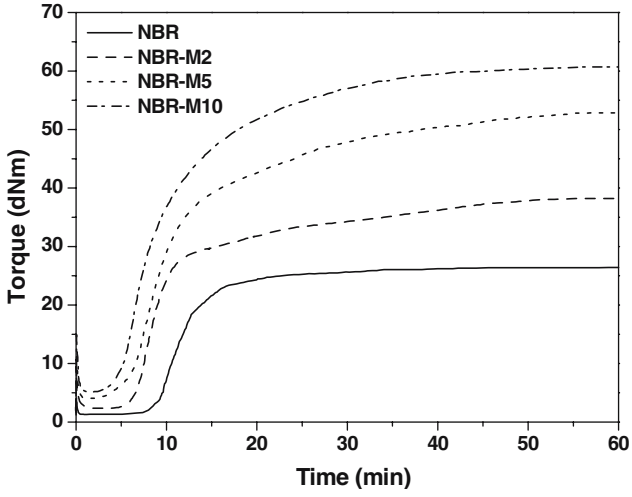

Fig. 2 Rheographic curves for NBR and NBR/Na-MMT with different loadings of Na-MMT at 160 °C

Tensile properties

It has been demonstrated that the complete dispersion of clay nanolayers in a polymer optimizes the number of available reinforcing elements carrying an applied load and deflecting cracks [11]. Interaction between the clay platelets having large surface area and the polymer chains facilitates stress transfer to the reinforcement phase, resulting in improved tensile properties. The stress-strain curves of cured NBR/Na-MMT nanocomposites are shown in Fig. 3a. The numerical values of mechanical properties are given in Table 2. NBR/Na-MMT nanocomposites showed a remarkable enhancement in engineering modulus and ultimate tensile strength, which were proportional to the clay content. There was a steep rise in tensile strength even with the addition of 2 phr of clay. NBR with 10 phr of Na-MMT showed about 5 time increase in tensile strength compared to pure NBR vulcanizate. The increase in modulus of clay filled nanocomposites may be related to the extent of exfoliation in presence of the dichloroacetic acid which was used as an electrolyte for coagulation. Kojima et al. [29] reported that the extent of exfoliation and its influence on Young's modulus was affected by the acid used as a catalyst for

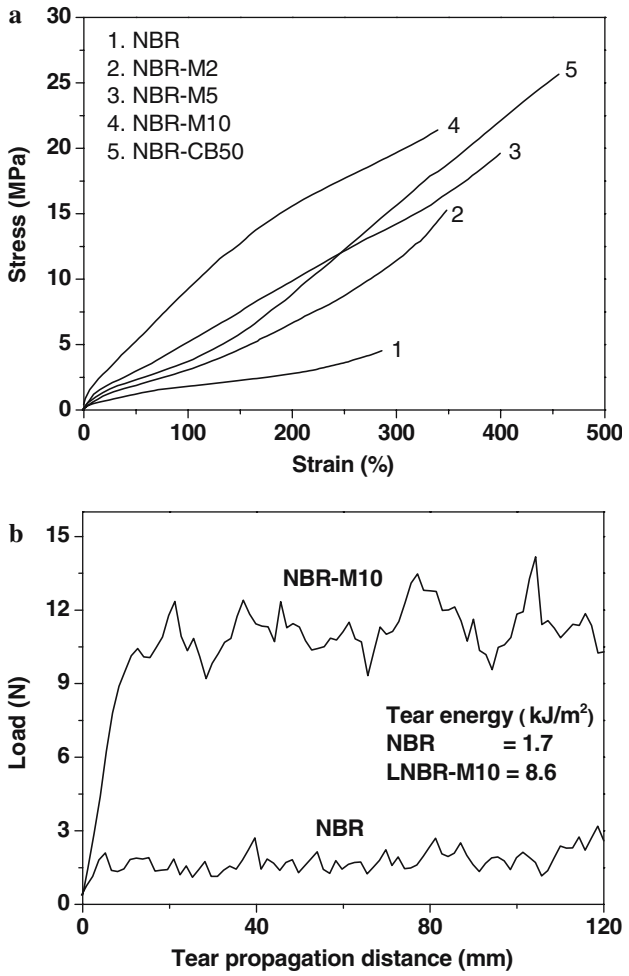

Fig. 3 (**a**) Stress–strain curve for NBR and its nanocomposites (a curve for NBR-CB50 is also included for comparison). (**b**) Plot of tear force vs. displacement for pure NBR and NBR-M10

polymerization of ϵ-caprolactam. Similarly, in the present system, the DCA had some influence on the degree of exfoliation. In contrast to the conventional rubber composite, which normally shows opposing effect of strength to modulus, the NBR/Na-MMT nanocomposites exhibited simultaneous improvement in ultimate strength and modulus. To our knowledge, there is no reported work on NBR nanocomposites containing small amount pristine clay possessing a tensile strength of greater than 20 MPa. Wu et al. reported the enhancement of tensile strength up to 18 MPa for 30 phr clay filled nanocomposite prepared from aqueous clay dispersion containing some compatibilizer [20]. The key factor for the improvement in the tensile properties was due to good dispersion and planar orientation of nanometric clay layers. The formation of good interfacial interaction between clay layers and polymer through polar interaction could have also increased the values of stress at break. The stiffness of the clay layers contributed to the immobilization of rubber phase as discussed by Eisenberg [30]. However the elongation at break of the nanocomposite increased with increasing clay content up to 5 phr and then decreased. The reduction in the elongation at break at higher loading may be attributed to the formation of clay tactoids, which effectively weaken the number of available reinforcing links. The effect of clay loading on tearing energy is listed in Table 1 for all samples and a representative plot is shown in Fig. 3b. The tearing energy of the nanocomposite increased with increase in clay loading, which was similar to tensile properties. The mechanism for improved tear resistance has been discussed in detail by Nah et al. [21]. The tear morphology of torn surface of NBR-M10 (Fig. 4a) showed a tear pattern clearly different from those of conventional composites, which normally shows the presence of cross-hatched pattern with numerous webs and steps of different sizes [21]. The tear pattern of the nanocomposites showed series of tear ridge parallel to the tearing direction, whereas the unfilled NBR showed simple torn surface without complexity (Fig. 4b). The tear propagated at a particular fashion resulting in tilting of tear lines with respect to tearing direction. The uniformly dispersed clay layers and small tactoids alter the tear path along their length depending on the orientation of clay layers. This leads to more resistance for tear propagation and hence higher tearing energy.

Aging resistance

The effect of thermal aging on rubber properties is considered to be primary important for the industrial applications for heat resistance purpose. The nitrile

Table 2 Dynamic storage modulii of the samples at various temperatures and T_g

Samples	E' (MPa) at					T_g (°C)	tan δ_{max}
	–50 °C	T_g	0 °C	50 °C	100 °C		
NBR	2191	27.93	3.941	2.741	2.273	–13.7	1.85
NBR-M2	2784	98.25	10.20	5.176	4.007	–12.6	1.47
NBR-M5	3599	153.6	21.02	10.38	7.266	–10.2	1.21
NBR-M10	4252	218.4	50.23	18.41	11.03	–9.03	0.91
NBR-CB50	3949	182.0	37.16	13.92	8.590	–14.2	0.93

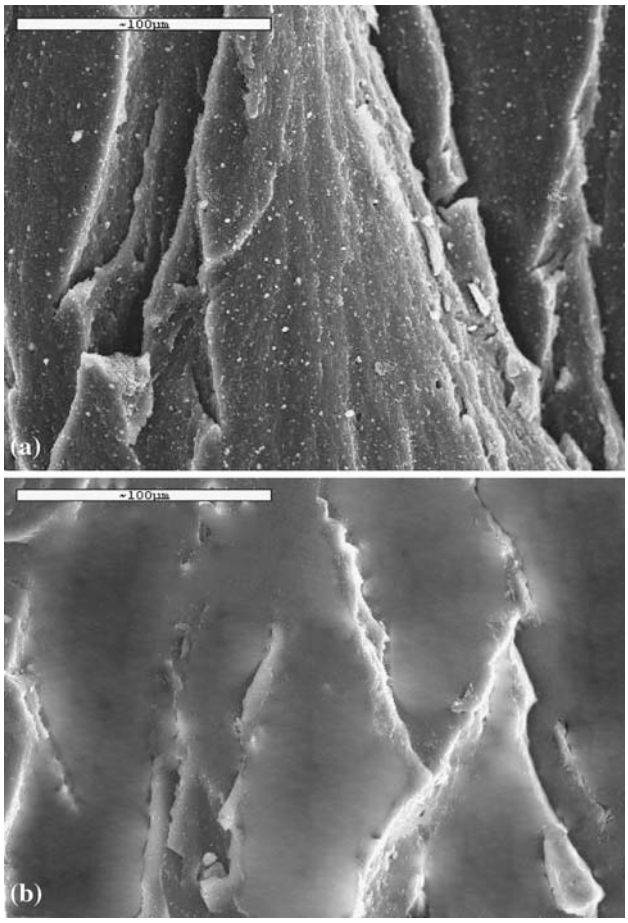

Fig. 4 SEM image of torn surface of (**a**) NBR-M10 and (**b**) pure NBR

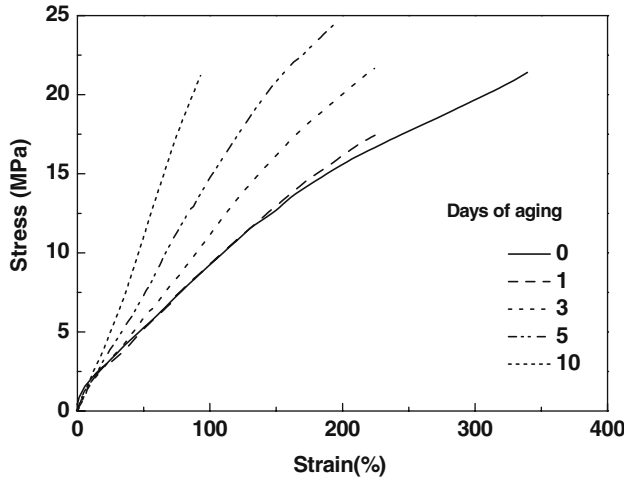

Fig. 5 Stress–strain curves of NBR-M10 aged for various time periods

rubber has good resistance towards oils and posses low gas permeability. Its use in automotive application is increasing. However, the heat aging resistant of NBR is limited because of the presence of unsaturated backbone. Inclusion of some heat barrier materials such as inorganic layered clay material may slowdown the aging process by controlling the diffusion of aging products from the outer surface into the interior. So the effect of thermal aging was investigated for the NBR/Na-MMT nanocomposites at 104 °C for 1, 3, 5 and 10 days. Figure 5 shows representative tensile curves of thermally aged NBR/Na-MMT nanocomposite containing 10 phr of clay. It is seen that, aging increased the modulus and hardness of the nanocomposite drastically with a considerable reduction in elongation. This behavior is a typical nature of any rubber compound, in which the modulus increase is observed due to the formation of more crosslinks. The tensile strength dropped at the beginning of aging and then increased and once again went down. It has been shown that the thermal aging of NBR is faster at the beginning of the aging due to higher level of oxygen uptake for oxidation [31] followed by crosslinking [32]. The oxidation resulted in partial degradation of polymer chain leading to reduction in tensile strength. However, upon continuation of aging, higher level of crosslinking lead to increase in tensile strength until there was a critical level of crosslinking beyond which the tensile strength dropped again due to restriction in chain flexibility. Figure 6a compares the trend in tensile strength of nanocomposites with carbon black filled system aged for different time periods. It is clearly seen that the nanocomposites were superior to conventional composite especially with 5 and 10 phr loading of Na-MMT in retaining the tensile strength. There was practically no loss of tensile strength of these nanocomposites where as NBR/CB composite lost much of its tensile strength after 10 days of aging. The clay layers might have acted as barriers for the diffusion of degradation products entering into the interior of the rubber product. However the loss in elongation at break after aging (Fig. 6b) may be due to increase in crosslinking density upon aging which lead to restriction for chain extension and decrease in chain length between crosslinking points.

Dynamic mechanical properties

The viscoelastic behavior of a filled polymer under dynamic loading condition can reveal the microstructure of the composite. The DMA is often used to study the viscoelastic characteristics and relaxations in the polymers and polymer composites. The dynamic mechanical properties as a function of temperature for pure NBR, NBR-CB50 and NBR/Na-MMT

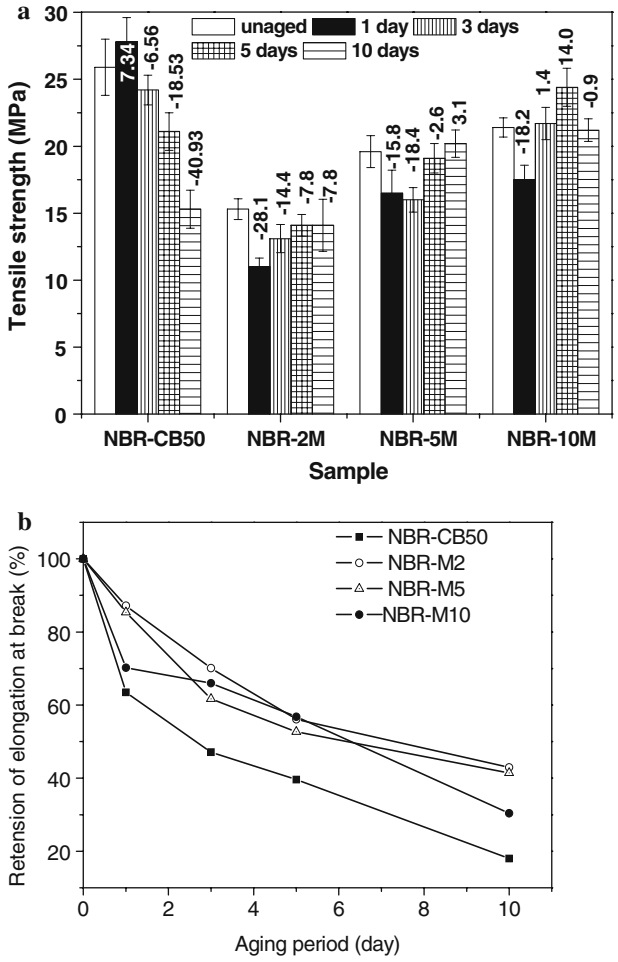

Fig. 6 (**a**) Comparison of tensile strengths of unaged and aged NBR and NBR/Na-MMT nanocomposites. The numbers over the bars represent the percent retention of tensile strength after aging for specified period. (NBR-CB50 is also included for comparison). (**b**) Comparison of percent retention of elongation at break of various samples

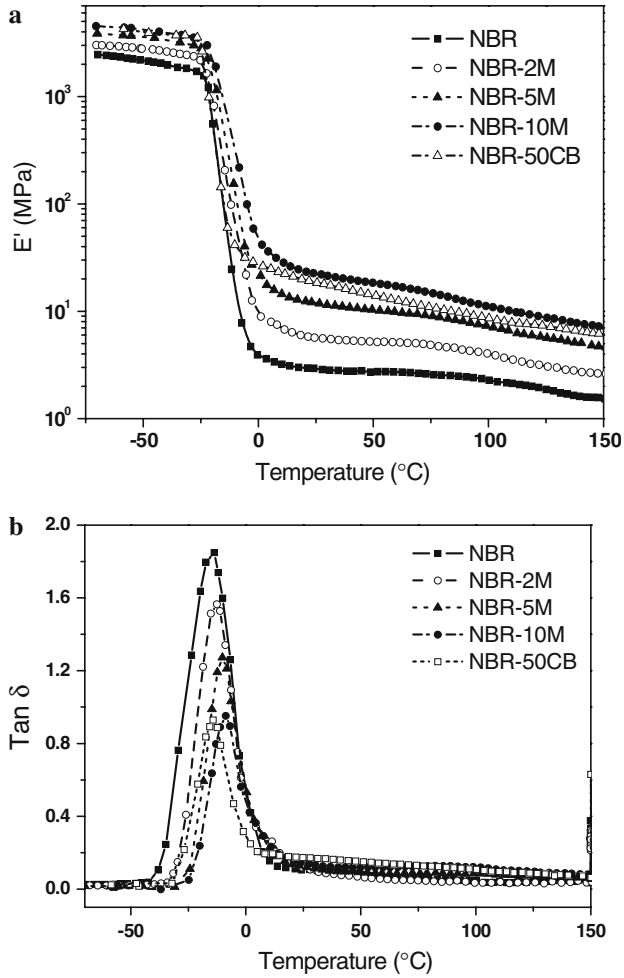

Fig. 7 (**a**) Storage modulus (E') versus temperature for NBR and its nanocomposites (The E' curve for NBR-CB50 is also included for comparison). (**b**) loss tangent (tan δ) versus temperature for NBR and its nanocomposites and (The tan δ curve for NBR-CB50 is also included for comparison)

nanocomposites with different clay loadings are shown in Fig. 7. In Fig. 7(a) the storage modulus of the NBR/Na-MMT nanocomposites increased with the increase in Na-MMT content in the temperature range of –70~150 °C. The results clearly showed that the addition of Na-MMT into NBR matrix resulted in a remarkable increase in the stiffness of material indicating reinforcing effect of Na-MMT. Specifically, the largest increase in the storage modulus of these nanocomposites was observed for NBR-M10 which was almost two and five times larger than that of pure NBR at –50 °C and 100 °C, respectively. Moreover, the E' of NBR-CB50 was lower than that of NBR-M10 as seen from Table 2. This reinforcement should increase the thermo-mechanical stability of the material at higher temperature. The loss tangent (tan δ) curves of the samples, representing the damping characteristic of the composites, are shown in Fig. 7(b). It is seen that tan δ peak of the nanocomposites representing glass transition were shifted from –13.7 °C for pure NBR to higher temperatures proportional to the Na-MMT loading (Table 2). However, no change in T_g of NBR-CB50 was observed. Generally, strong interactions between the nanolayers and the matrix polymer can restrict the movement of polymer segments near to the filler surface, thus resulting in an increase of the glass transition temperature of the matrix [33]. The tan δ curves of the NBR/Na-MMT nanocomposites were very much similar to that of pure NBR except that there was considerable reduction in the tan δ peak height for pure NBR. Upon increasing the level of Na-MMT, the peak height became small, indicating the restriction in damping characteristics of Na-MMT filled NBR.

To investigate the effect of Na-MMT on dynamic mechanical properties, the area under tan δ peak, related to the activation enthalpy of relaxation of the backbone motion of the polymer chain was analyzed. For example, the average activation enthalpy of transition for polymers and their composites can be calculated from the dynamic mechanical data [34] using following equation.

$$t_A = \frac{(\ln E_G - \ln E_R)\pi R T_g^2}{2(\Delta H_a)_{avg}} \quad (4)$$

where t_A is area under tan δ curve, and E_G and E_R, are the storage modulus at glassy phase and rubbery phase, respectively. $(\Delta H_a)_{avg}$ is the activation enthalpy of the transition process. Accordingly, t_A value is dependent on both the height and width of the tan δ peak, which is related to chain mobility and different relaxation processes contributing to the overall transition. The area under tan δ peak (t_A) and the activation enthalpy of transition of the blends having different compositions are given in Table 3. When Na-MMT was dispersed in NBR, the tan δ peak height was reduced leading to decrease in t_A. According to the Eq. 4, there is an inverse relationship between t_A and $(\Delta H_a)_{avg}$. So, any change in t_A values results in opposite effect in the enthalpy of activation. Hence, the $(\Delta H_a)_{avg}$ of NBR/Na-MMT nanocomposite was increased indicating the restriction of chain mobility in the composite due to stiffening of polymer chains enclosed between the clay layers leading to change in damping characteristics. It is seen from the Table 3 that the increase in $[(\Delta H_a)_{avg}]_{NBR}$ was proportional to the Na-MMT content.

Correlation of relaxation phenomena with physical model

The relaxation of the polymer chains at the glass transition can be explained by molecular model for the deformation of an amorphous polymer near T_g. This model has been applied to describe the influence of fillers on molecular restriction in amorphous, semicrystalline polymers and composites. Hence, the complex modulus (E^*) can be expressed by [35]

$$E^* = E_R + \frac{E_G - E_R}{1 + H(i\omega\tau)^{-h} + (i\omega\tau)^{-k}} \quad (5)$$

where E_R is the modulus of the polymer in rubbery state, E_G the modulus of the polymer in glassy state, ω the angular frequency, τ the relaxation time at the glass transition, i the imaginary number ($\sqrt{-1}$) k ($0 < k < 1$) and h ($0 < k < h < 1$) are the parameters related to segmental mobility of the chains and physical and/or chemical crosslinks, respectively. H is the function of k and h.

The different parameters in the above equation can be determined from Cole–Cole plot (Fig. 8) obtained by plotting E'' vs. E'. The h and k were obtained from the slopes of the Cole–Cole diagrams corresponding respectively to lower and higher temperatures, i.e. they were obtained from the angles (θ_G, θ_R) between the tangent and the E' axis. E_G and E_R were obtained by extending this tangent onto the E' axis to lower and higher temperatures, respectively. The way to determine each of these parameters is explained in the literature [35].

The parameter values, so obtained for the NBR/Na-MMT systems, are given in Table 3. The presence of Na-MMT decreased both h and k values. Here, h decreased from 0.90 to 0.64 and k from 0.66 to 0.58. The decrease in these parameters resulted from reduction in segmental mobility of polymer chain and strong interaction at the interface between clay layers

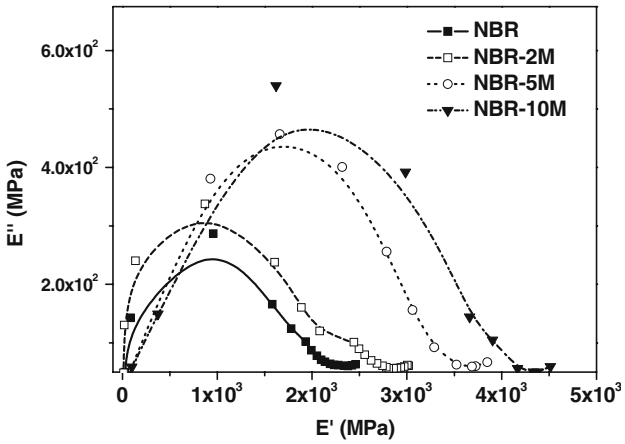

Fig. 8 Cole–Cole plot of pristine NBR and NBR/clay nanocomposites with different filler loading

Table 3 The area under tan δ peak, average activation enthalpy of transition and the model parameters of NBR and its nanocomposites

Samples	t_A	E_G	E_R	$(\Delta H_a)_{avg}$ kJ/mol	θ_R	θ_G	$h = 2\theta_R/\pi$	$k = 2\theta_G/\pi$
NBR	26.62	2459.7	2.181	473.7	81.03	59.04	0.902	0.660
NBR-M2	24.63	3019.5	3.520	491.7	79.02	58.01	0.876	0.639
NBR-M5	21.83	3849.0	6.011	534.9	71.76	55.00	0.803	0.610
NBR-M10	16.47	4513.3	11.57	666.7	66.64	52.53	0.737	0.576

and polymer matrix. These predictions are in accordance with the reduction in damping peak area obtained from DMA analysis. Also, the SEM image of torn surface of nanocomposite showed rough fractured surface indicating good adhesion between polymer and filler.

In order to correlate the variation in storage modulus with respect to the volume fraction Na-MMT at different temperatures, a simple model equation is proposed. Thus

$$E'_c = E'_o(1 + B\phi_f)^C \quad (6)$$

where E'_c and E'_o = storage modulus of the composite and matrix, respectively ϕ_f is the volume fraction of clay, B and C are the temperature dependant fitting parameters related to the magnitude of change in the modulus (relaxation phenomena). The curves in Fig. 9a compare storage modulus of nanocomposites (E'_c or E') versus volume fraction of Na-MMT obtained from experimental results and model equation. Interestingly, there was no much deviation between experimental and the model values indicating the suitability of model for prediction of storage modulus of nanocomposite. The variation of model parameters B and C against temperature (Fig. 9b) suggested that both B and C attained highest values close to the glass transition temperature, where there is a maximum relaxation of chain molecules.

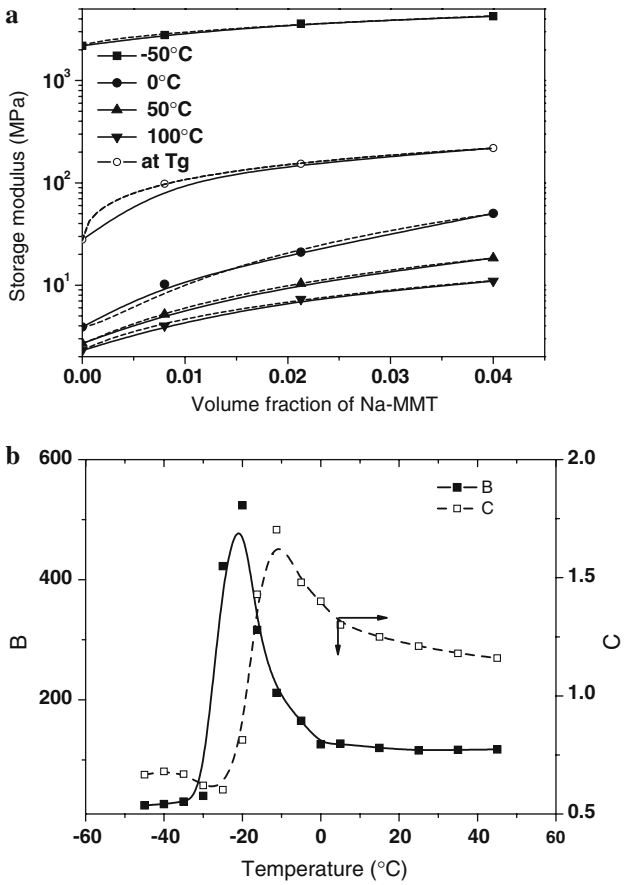

Fig. 9 (**a**) Comparison between experimental and calculated E' for NBR and its nanocomposites at different temperatures. (**b**) Variation of model parameters B and C with temperature

Differential scanning calorimetry

The differential scanning calorimetric (DSC) curves of pure NBR and NBR/Na-MMT nanocomposites are given in Fig. 10. The DSC thermogram of NBR showed the glass transition (T_g) at –22.0 °C whereas the nanocomposite showed the heat inflection at higher temperature with an increase of about 10 °C for NBR-M10. This increase in T_g of nanocomposites is in accordance with the results obtained from DMA. The increase in T_g of the nanocomposites might be due to (i) the effect of a small amount of dispersed clay on the free volume of polymer and (ii) the confinement of the intercalated/exfoliated polymer chains within the clay galleries which resists the segmental motion of the polymer chains [36].

Thermogravimetric analysis

Figure 11 shows the thermogravimetric (TG and DTG) curves for NBR and its nanocomposites containing 5 and 10 phr Na-MMT. The initiation of degradation of pristine NBR was found to occur at around 367 °C and maximum degradation occurred at

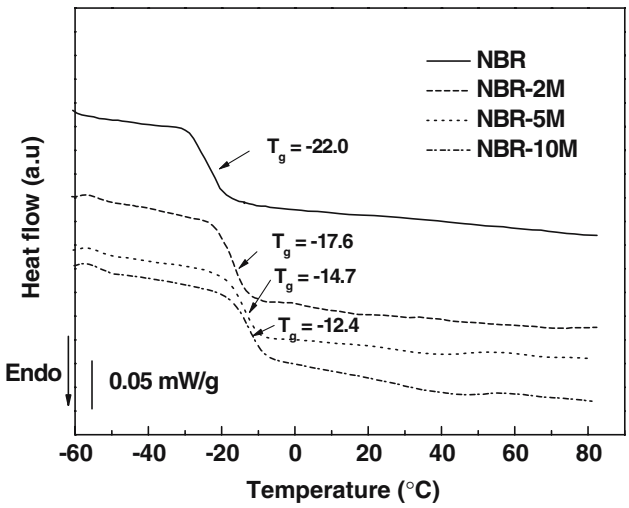

Fig. 10 DSC thermogram of NBR and its nanocomposites with different clay loading. The glass transition temperature (T_g) of samples are indicated by arrows. The heating rate of 10 °C/min is used for all samples

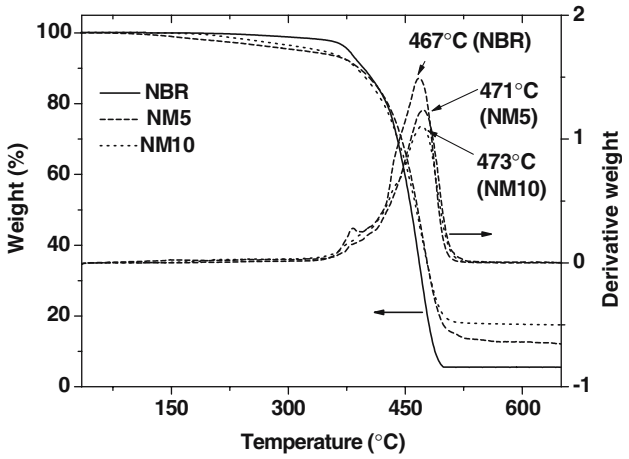

Fig. 11 Thermogravimetric curves (TG and DTG) of NBR and its nanocomposites

467 °C. The incorporation of Na-MMT into the NBR decreased the initiation of degradation due to the presence of residual electrolyte of low molecular weight. However, the maximum degradation temperatures were slightly increased to 471 and 473 °C for NBR-5 M and NBR-10 M, respectively. It is generally believed that the inclusion of inorganic components into organic materials can improve their thermal stability [37]. The presence of residue beyond 600 °C in the TGA curves is due the presence of compounding ingredient (in this case, ZnO) and the inorganic clay in nanocomposites. The observed increase in the thermal stability of NBR/Na-MMT may be due to the high thermal stability of clay and the interaction between the clay layers and the polymer matrix through intercalation/exfoliation. These intercalated polymer chains were covered by clay layers which prevents direct exposure of these chains to thermal influence.

Conclusions

NBR/layered clay nanocomposites were successfully prepared through latex blending of unmodified clay dispersion and NBR latex. The XRD characterization of nanocomposites showed the existence of intercalated/exfoliated structure. The TEM images revealed the presence of well dispersed clay layers in the NBR matrix together with only some tactoids containing few layers of clay. The vulcanization characteristics of NBR/clay hybrids were altered by reducing scorch time and increasing minimum and maximum torque values without affecting optimum cure time. The nanocomposites showed remarkable improvements in modulus, hardness and strength properties due to high level of clay dispersion. Additionally, the retention of tensile properties of the nanocomposites after 10 days of air aging was superior to conventional carbon black filled composite with high filler loading. The dynamic storage moduli of NBR/clay nanocomposites are significantly larger than that of pure NBR due to confinement of part of polymer chains between clay layers. The damping characteristics of nanocomposites were noticeably reduced and the magnitude of reduction was correlated with a physical model. The proposed linear equation to correlate the clay loading with damping of nanocomposites at various temperatures gave good fitting with experimental results proving the suitability of the model equation. The glass transition temperatures of nanocomposites measured by DSC increased with increase in clay loading. There was a little improvement in the thermal stability of nanocomposites even at with 10 phr of clay loading.

Acknowledgements This work was supported by the program for cultivating graduate students in regional strategic industry (2003) and by the grant of Post-Doc. Program, Chonbuk National University (2004).

References

1. Vaia RA, Price G, Ruth PN, Nguyen HT, Lichtenhan J (1997) J Appl Clay Sci 15:67
2. Messersmith PB, Giannelis EP (1995) J Polym Sci; Polym Chem 33:1047
3. Yano K, Usuki A, Okada A, Kurauchi T, Kamigaito O (1993) J Polym Sci; Polym Chem 31:2493
4. Kojima Y, Usuki A, Kawasumi M, Okada A, Kurauchi T, Kamigaito O (1993) J Appl Polym Sci 49:1259
5. Messersmith PB, Giannelis EP (1995) J Polym Sci; Polym Chem 33:1047
6. Theng BKG (1979) Formation and properties of clay–polymer composites-development in soil science. Elsevier Scientific Publishing Corp, Amsterdam
7. Alexandre M, Dubois P (2000) Mater Sci Eng 28:1
8. Vaia RA, Teukolsky RK, Giannelis EP (1994) Chem Mater 6:1017
9. Karger-Kocsis J, Wu CM (2004) Polym Eng Sci 44:1083
10. Ray SS, Okamoto M (2003) Prog Polym Sci 28:1539
11. Lebaron PC, Wang Z, Pinnavaia T (1999) J Appl Clay Sci 15:11
12. Hwang W-G, Wei K-H, Wu C-M (2004) Polymer 45:5729
13. Wang Y-Z, Zhang L-Q, Tang C-H, Yu D-S (2000) J Appl Polym Sci 78:1879
14. Wu Y-P, Wang Y-Q, Zhang H-F, Wang Y-Z, Yu D-S, Zhang L-Q, Yang J (2005) Comp Sci Technol 65:1195
15. Varghese S, Karger-Kocsis J (2003) Polymer 44:4921
16. Varghese S, Gatos KG, Apostolov AA, Karger-Kocsis J (2004) J Appl Polym Sci 92:543
17. Kim J-T, Oh T-S, Lee D-H (2003) Polym Int 52:1203
18. Nah C, Ryu HJ, Kim WD, Chang YW (2003) Polym Int 52:1359
19. Kojima Y, Fukumori K, Usuki A, Okada A, Kurauchi T (1993) J Mater Sci Lett 2:889
20. Wu Y-P, Jia Q-X, Yu D-S, Zhang L-Q (2003) J Appl Polym Sci 89:3855

21. Nah C, Ryu HJ, Han SH, Rhee JM, Lee MH (2001) Polym Int 50:1265
22. Kim JT, Oh TS, Lee DH (2004) Polym Int 53:406
23. Okada A, Usuki A, Kurauchi T, Kamigaito O (1995) In Mark JE, Lee CYC, Bianconi PA (eds) Hybrid organic-inorganic composites. ACS Symp Ser
24. Chen M, Ao N-J, Chen Y, Yu H-P, Qian H-L, Wang C, Zhou H-L, Qu J-L, Guo C-K (2001) J Appl Polym Sci 82:338
25. Choi DC, Kader MA, Cho B-H, Huh Y-I, Nah C. (2005) J Appl Polym Sci 98:1688
26. Gent AN, Henry AW (1968) Proceedings of international rubber conference. MacLaren and Sons London p 193
27. Hackett E, Manias E, Giannelis EP (1998) J Chem Phys 108:7410
28. Best LL, Morrell SH (1955) Rubber Chem Technol 28:1185
29. Kojima Y, Usuki A, Kawasumi M, Okada A, Kurauchi T, Kamigato O (1993) J Polym Sci; Polym Chem 31:1755
30. Tsagaropoulos G, Eisenber A (1995) Macromolecules 28:6067
31. Morrell PR, Patel M, Skinner AR (2003) Polym Test 22:651
32. Delor-Jestin F, Barrois-Oudin N, Cardinet C, Lacoste J, Lemaire J (2000) Polym Degrad Stabl 70:1
33. Huang HH, Wilkers GL, Carlson JG (1989) Polymer 30:2001
34. Lin M, Lee S (1997) Polymer 38:53
35. Bergeret A, Alberola N (1996) Polymer 37:2759
36. Lu H, Nutt S (2003) Macromolecules 36:4010
37. Wen J, Wikes GL (1996) Chem Mater 8:1667